Geofísica Internacional (1996), Vol. 35, Num. 3, pp. 285-300

Crustal structure of the southeastern Brazilian continental margin from surface wave dispersion

Jorge Luis de Souza
Observatório Nacional, Departamento de Geofísica, Rio de Janeiro, Brasil.

RESUMEN

Las curvas de dispersión continentales se obtuvieron de las velocidades de grupo de ondas de Rayleigh para seis sismos con epicentros en el Atlántico Sur. La inversion sugiere una corteza superior sedimentaria, con velocidades de S de 1.32-2.90 km/s, seguida por un basamento cristalino de 3.06-3.38 km/s. La corteza inferior es transicional (4.02-4.22 km/s) como en otros bordes continentales pasivos. La base de la corteza se encuentra a 36±4 km pero existen valore menores en los perfiles A a C.

PALABRAS CLAVE: Dispersión de ondas de Rayleigh, velocidad de ondas S, margen continental de Brasil.

ABSTRACT

Source-station Rayleigh wave group velocities are decomposed to obtain pure continental shelf dispersion curves along three profiles. Inversion results of these dispersion curves indicate that the upper crust is dominated by sediments and high velocity sedimentary rocks with shear wave velocities varying from 1.32 to 2.90 km/s. The intermediate crustal layer has assumed shear wave velocities typical of crystalline basement ($3.06 \leq \beta \leq 3.38$ km/s). The lower crust seems to be composed of a transitional layer ($4.02 \leq \beta \leq 4.22$ km/s), similar to those observed at other passive continental margins (e.g., Dainty *et al.*, 1966; Calcagnile *et al.*, 1982). These results are in agreement with those of a recent surface wave study conducted in the same area (Souza, 1995). Moho boundary is clearly defined around 36±4 km depth, but a reduction in the crustal thickness is observed from profile A to C.

KEY WORDS: Rayleigh wave dispersion, shear wave velocity, southeastern Brazilian continent margin.

INTRODUCTION

The low density and the irregular distribution of seismological stations along the coast of the continents surrounding the Atlantic Ocean have been the main factors for the poor knowledge of the Earth's interior in both the central and southern parts of the Atlantic Ocean. Despite several global seismological investigations in the Atlantic Ocean area (Honda and Tanimoto, 1987; Mocquet *et al.*, 1989; Mocquet and Romanowicz, 1990), knowledge of the physical properties of the lithosphere in this region is still limited owing to the poor distribution of stations and, consequently, poor lateral resolution.

It is well known that source-station dispersion curves have successfully contributed to study of the lithosphere's evolution into Atlantic and Pacific Oceans (Weidner, 1974; Forsyth, 1975; Canas and Mitchell, 1981). In the south Atlantic region, the Brazilian seismological station RDJ (Figure 1) can be used to provide similar information. Because RDJ is located in a geographical position which allows for the detection of a large part of the seismicity of the south Atlantic Ocean in a wide azimuthal range, it is ideal to study the region through surface wave dispersion curves.

The main goal of this paper is to obtain the S-wave velocity structures for the southeastern Brazilian continental shelf region using surface wave dispersion curves obtained at Brazilian seismological station RDJ (Rio de Janeiro).

DATA PROCESSING

Six earthquakes which occurred in the South Atlantic Ocean are used in the determination of the surface wave dispersion curves. The location of epicenters and stations are shown in Figure 1. The geographical position of the epicenters suggests the formation of three groups of paths (A, B and C-Figure 1). The hypocentral parameters were obtained through Earthquake Data Reports Bulletins (Table 1).

The RDJ seismological station is equipped with three long-period seismometers, one vertical Sprengnether and two horizontals Press-Ewing, linked to analog recorders. The vertical components of motion are used to calculate the source-station Rayleigh wave group velocities. The analog seismograms were digitized at irregular intervals, and a sampling rate of 1 sample per second was obtained after linear interpolation. Instrumental correction was applied during the calculation of the source-station dispersion curves, using a multiple filter techniques (Dziewonski *et al.*, 1969).

DETERMINATION OF CONTINENTAL SHELF GROUP VELOCITIES

The objective of the present study is to investigate the S-wave velocity structure in the southeastern Brazilian continental shelf region. However, first it is necessary to compute a Rayleigh wave dispersion curve representative of that area, and therefore, decomposition of the total paths should be considered.

The process of decomposition of large surface wave paths into several segments representing different geological provinces has been widely applied in the literature

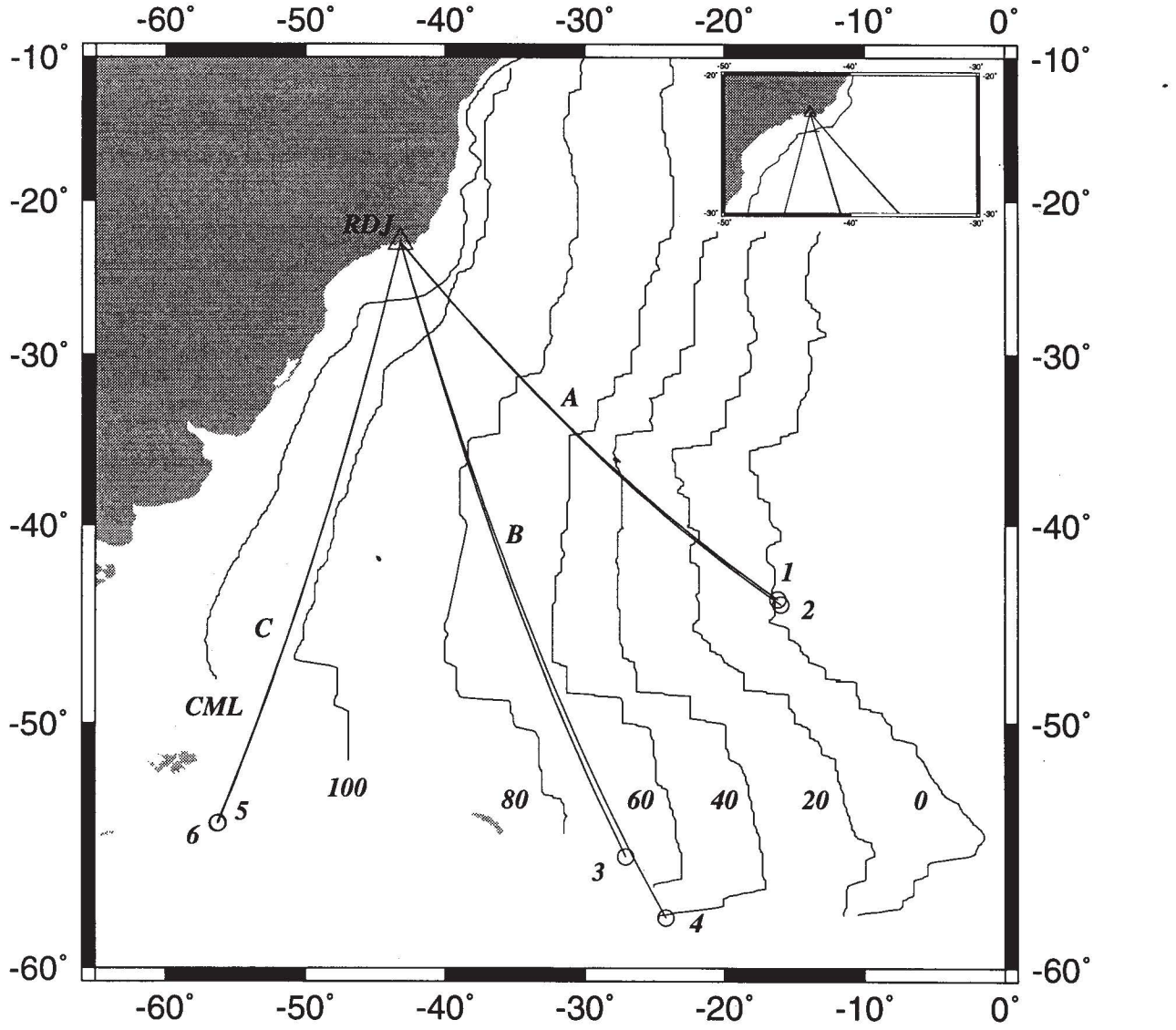

Fig. 1. Map showing the location of both epicentres and seismological station RDJ, Rayleigh wave paths for the groups (A, B and C) and the sea-floor age divisions from 0 to 100 Ma (Emery and Uchupi, 1984). The continental margin limit (CML) line is also displayed (Emery and Uchupi, 1984). A detail of the southeastern Brazilian continental margin is shown of the upper right side. Inside it, the bathymetric line contour of 400 m used as reference to split total surface wave paths.

(Santô, 1960; Santô and Bath, 1963; Forsyth, 1975; Christensen *et al.*, 1980). In the present study, the source-station paths were partitioned into two types of structures. The structure to be analyzed in this study has a fixed length of approximately 167 km (Figure 1). The 400 m bathymetric contour (Emery and Uchupi, 1984) was used as the reference in separating total paths into oceanic and continental shelf regions (Figure 1).

It is well known that Rayleigh wave group velocity of the continental shelf can be calculated through the expression

$$\frac{L_t}{U_t} = \frac{L_c}{U_c} + \frac{L_o}{U_o} \qquad (1)$$

where U_t is the group velocity for total path, U_c is the group velocity for the pure continental shelf path, U_o is the group velocity for the pure oceanic path, and L_t, L_c, L_o are the total, continental shelf and oceanic path lengths, respectively.

The major problem in using equation (1) is the lack of a specific oceanic model for the south Atlantic Ocean. There are in the literature several average oceanic models (Kanamori, 1970; Dziewonski, 1971; Anderson and Hart, 1976) which might be used to remove the oceanic effect from the mixed paths. However, these models are not appropriate for the present situation because they are based on global data which represent an average of all oceanic regions of the world. Souza (1994) has used the source-station dispersion curves of the earthquakes of this study to

Table 1

Hypocentral parameters of the earthquakes obtained from Earthquake Data Report Bulletins, along with epicentral distances (Δ) and back azimuths (BAz.) both in degrees (deg).

event NO.	date Y/M/D	origin time h min sec	latitude deg.	longitude deg.	depth km	magnitudes m_b	M_S	Δ deg.	BAz. deg.
1	81/11/16	05 00 45.96 ± 0.22 sec	43.967 S ± 6.5km	16.201 W ± 4.2km	10	5.3	5.1	30.60	139.87
2	82/11/13	15 11 18.07 ± 0.55 sec	44.232 S ± 17.6km	16.015 W ± 7.4km	10	4.8	-	30.86	140.14
3	82/11/08	09 44 06.99 ± 0.14 sec	55.767 S ± 4.2km	27.076 W ± 3.0km	33	5.3	5.3	34.94	164.07
4	83/01/29	15 29 17.93 ± 0.22 sec	58.151 S ± 6.9km	24.206 W ± 4.5km	42	5.1	5.5	37.79	163.62
5	82/11/18	00 27 50.79 ± 0.11 sec	54.377 S ± 2.5km	56.217 W ± 3.2km	10	5.7	5.4	32.92	194.01
6	82/11/19	10 57 35.46 ± 0.13 sec	54.415 S ± 3.4km	56.311 W ± 3.8km	10	5.6	4.8	32.98	194.07

investigate the S-wave velocity structure in the region (Figures 2-3). Considering that more than ninety per cent of the paths in his study are in a purely oceanic structure, it is reasonable to consider Souza's results as a reference in correcting for the oceanic structure. A similar procedure has been adopted by Souza (1995) to remove the oceanic effect from mixed dispersion curves in the south Atlantic Ocean.

Oceanic models were constructed to remove oceanic structures along the paths A, B and C. The average thicknesses of both water and sediments were obtained from charts IB (bathymetry) and VB (depth to basement) of Emery and Uchupi (1984). The average thicknesses of the first and second oceanic layers were also obtained from Emery and Uchupi (1984). The thicknesses of the other layers were obtained from the surface wave study of Souza (1994). The P-wave velocities of layers, 3, 4, 5, 6 and 7 (Table 2) are those of Souza (1994), owing to similarity between Souza's compressional wave velocities and those (chapter 3-Table 4) presented by Emery and Uchupi (1984). It must be emphasized that P-wave velocities from Souza' study were obtained through a well-known relationship between shear wave velocities and Poisson's ratio. The S-wave velocities are those of Souza (1994), except for the sedimentary layers which were not resolved in Souza' study. For these layers, an S-wave velocity of 1.00km/s was assumed. The densities for the oceanic crust were obtained from the Nafe-Drake relationship (Talwani *et al.*, 1959), and for the upper mantle from Birch's relation (Birch, 1964). The oceanic models for the three paths are shown in Table 2.

The Rayleigh wave group velocities of the continental shelf were computed using source-station dispersion curves (Figure 3), oceanic dispersion curves obtained from the models shown in Table 2 and equation (1). In order to get a dispersion curve representative of each path, a Chebyshev polynomial fit was applied. The result of this procedure is shown in Table 3.

Errors in group velocity measurements have been widely discussed in the literature (Chave, 1979; Cloetingh *et al.*, 1979). In the present study, the errors due to epicenter mislocation (Table 1), origin time (2s), source finiteness (3s), initial phase in the source (2s) rise time (1s) and standard deviation from Chebyshev polynomial fit are considered in the computation of the corresponding group velocity errors. All errors in the continental shelf dispersion curves were calculated assuming that the epicenters were located at the intersection between Rayleigh wave paths and the 400 m bathymetric contour (Figure 1). In other words, the epicentral distance used in the error determinations was 167 km. Moreover, the epicenter mislocation error was computed using only the largest value shown in Table 1. Total errors were then obtained from the root mean square sum of the errors cited above (Table 3).

INVERSION OF CONTINENTAL SHELF DISPERSION CURVES

The inversion process was divided into two steps. In the first step, the models are composed of many thin layers overlying an infinite half-space, so that the results can be used as a reference for another starting model. In the second step, groups of thin layers with the same features, normally similar shear velocities, are transformed into thick layers, so that another inversion is performed.

In the first step, all crustal models were divided into twelve 4 km thick layers overlying an infinite half-space.

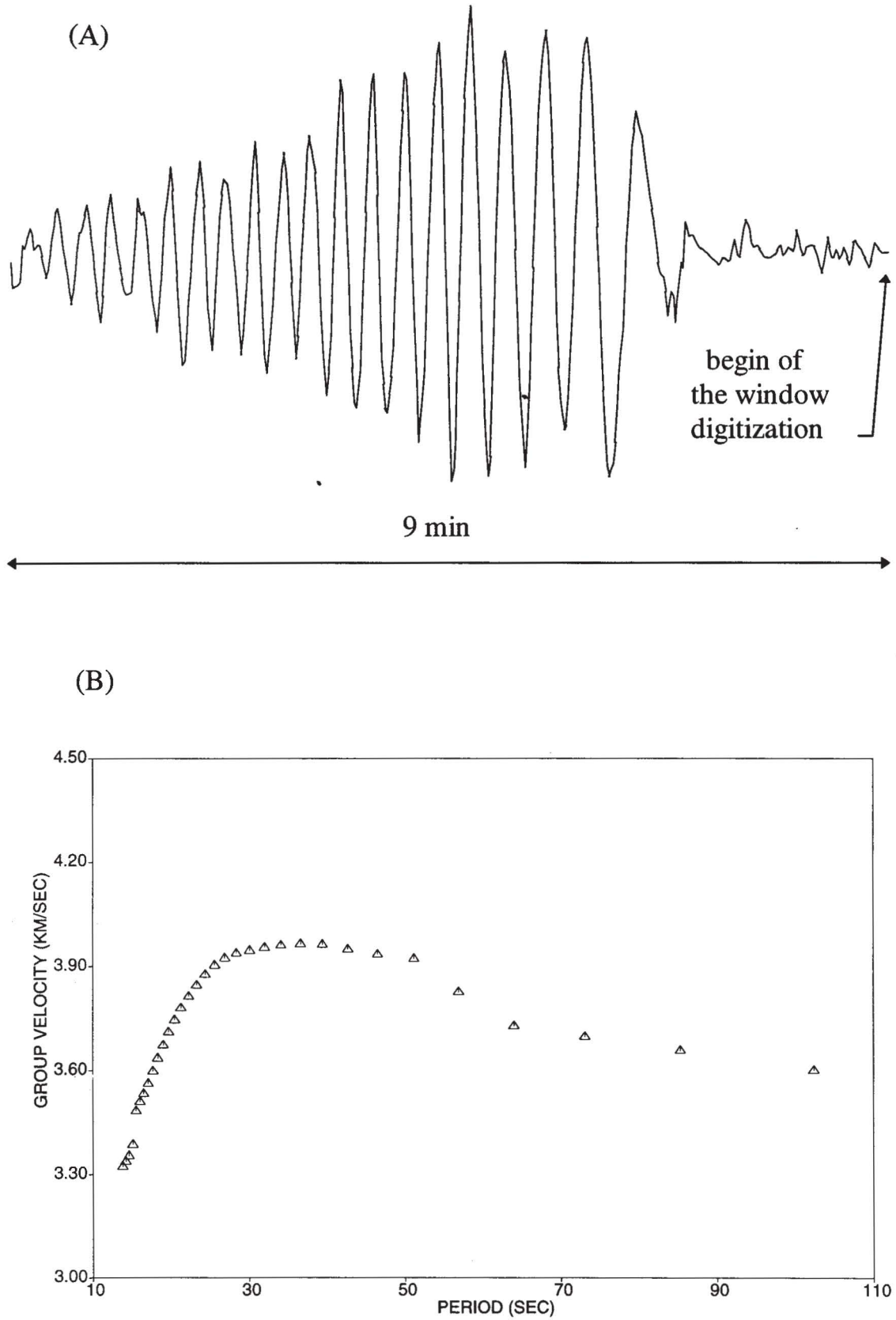

Fig. 2. Example of source-station data obtained at RDJ station. (a) Digital seismogram of the earthquake number 1 (Table 1) and respective duration of the signal. (b) Source-station Rayleigh wave dispersion corresponding to the seismogram displayed in (a).

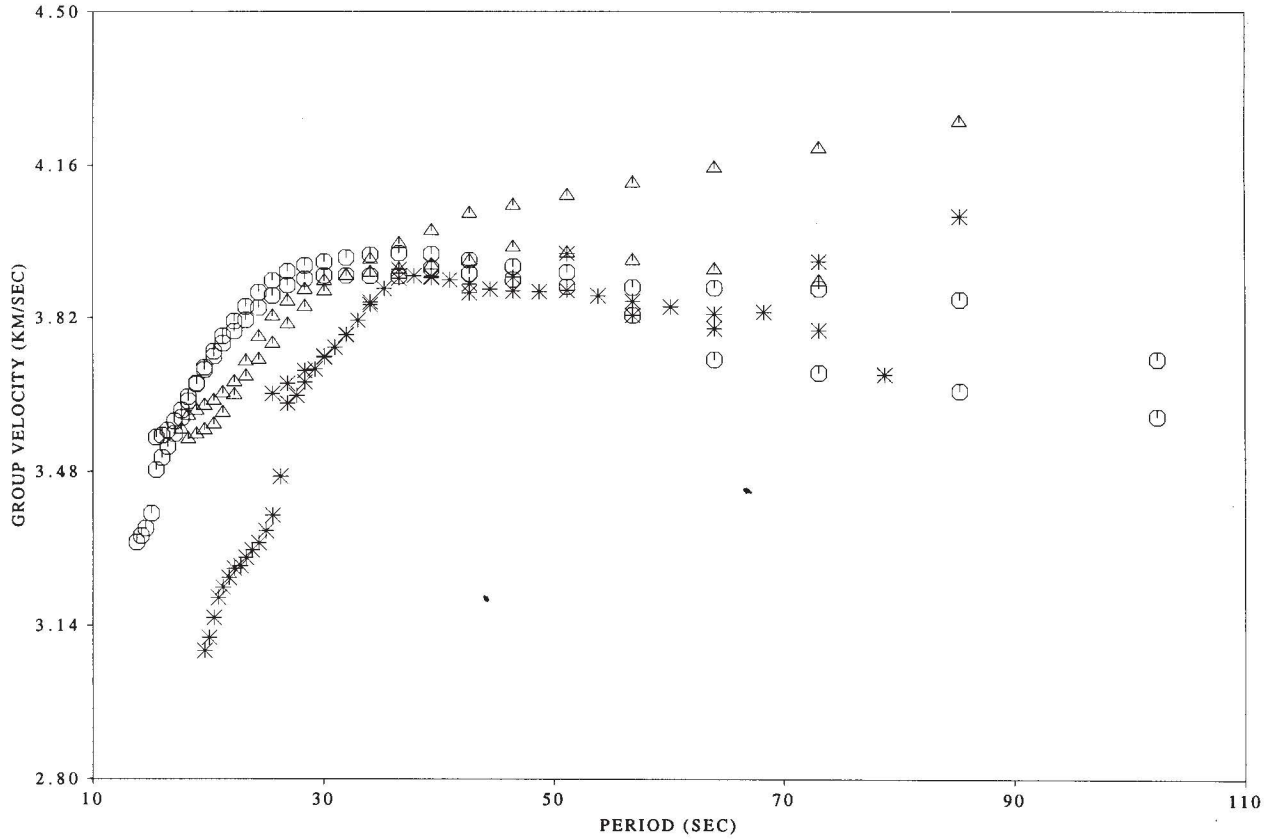

Fig. 3. Source-station Rayleigh wave group velocities for the six earthquakes used in the present study. Each symbol represents one path. Circles represent path A; triangles, path B; and asterisks, path C.

These starting models are composed of two parameters, a shear wave velocity (β) and a Poisson's ratio (σ). The inversion procedure for all models started with a S-wave velocity of 5.0km/s in both the crust and uppermost mantle, and a Poisson's ratio of 0.25 and 0.27 in the crust and upper most mantle, respectively (Tarkov and Vavakin, 1982).

The differential inversion method implement in the computer program SURF (Herrmann, 1991) was applied in the determination of the S-wave velocity structures in the southeastern Brazilian continental shelf. Inversion results will be displayed and discussed in the next section.

DISCUSSION AND INTERPRETATION

Inversion results for the first step are shown in Figures 4-6. The theoretical (solid line) and calculated (triangles) Rayleigh wave group velocities are shown in Figures 4a, 5a and 6a. The estimated shear wave velocity structures with corresponding resolving kernels are shown in Figures 4b, 5b and 6b. Table 4 also shows the estimated shear wave velocity structures, along with the standard deviations of these measurements for the three paths (A, B and C).

As expected, the inversion results are characterized by groups of layers with shear velocities slightly similar to one another. In the path A (Figure 4b), three well defined velocity gradients are observed at 12, 20 and 44 km depth, which can be related to the following transitions: the sediments-crystalline basement transition (from 2.81 to 3.32 km/s), the crystalline basement-transitional layer transition (from 3.32 to 4.03 km/s) and the transitional layer-uppermost mantle transition (from 4.22 to 5.00 km/s), respectively. The Moho is clearly indicated by the velocity gradient at 44 km. As continental shelves are commonly characterized by crustal thickness varying from 30 to 35 km, the crust here is anomalously thick. This result is consistent with a recent surface wave study in the southeastern Brazilian continental shelf (Souza, 1995) which, although it did not, sharply define the crust-mantle transition, indicated that Moho was around 40±5 km. Another aspect also observed both in the present study and Souza' study is the existence of a transitional layer in the lower crust (Table 4). In the present study this layer becomes more significant that in Souza' study, probably due to the wide period range of the dispersion curves. Transitional layers have been found in other passive continental margins in Canada (Dainty *et al.*, 1966) and in the Mediterranean area (Calcagnile *et al.*, 1982). In the case of the Mediterranean area, Calcagnile *et al.* (1982) associated shear wave velocities ranging from 4.0 to 4.2 km/s with transitional layers. This velocity range is exactly the same observed in the path A (Table 4). Similarly, P-wave velocities related to

Table 2

Earth's models used to remove oceanic structures along of the three paths (A, B and C). α is compressional wave velocity , β is shear wave velocity and ρ is density.

thickness (km)	α (km/s)	β (km/s)	ρ (g/cm^3)
	PATH A		
3.0	1.52	0.00	1.03
0.7	2.10	1.00	2.10
1.9	5.17	2.99	2.53
3.5	6.75	3.90	2.91
30.0	7.62	4.40	3.13
20.0	7.91	4.57	3.24
∞	6.91	3.99	2.86
	PATH B		
3.0	1.52	0.00	1.03
0.7	2.10	1.00	2.10
1.9	5.23	3.02	2.54
3.5	6.80	3.93	2.93
30.0	7.65	4.42	3.14
20.0	8.08	4.67	3.31
∞	7.67	4.43	3.15
	PATH C		
5.4	1.52	0.00	1.03
3.0	2.10	1.00	2.10
1.9	5.42	3.13	2.58
3.5	6.87	3.97	2.95
30.0	7.56	4.37	3.11
20.0	8.31	4.80	3.39
∞	7.29	4.21	3.01

the transitional layer displayed in Table 4, (vary from 6.99 to 7.52 km/s). These velocities were calculated from a well-known relationship between P wave (α), S wave (β) and Poisson's ratio (σ) assuming σ=0.25 for the crust (Tarkov and Vavakin, 1982). As these velocities are similar to those found by Dainty *et al.* (1966) ($7.08 \leq \alpha \leq 7.53$ km/s), for the crustal transition layer we consider these results as another evidence to support this interpretation. The resolving kernels associated with path A are somewhat poor in the whole crust, due to reasonable value of the damping parameter (0.1) used in the inversion process. The best results were at around 10 km depth and in the half-space. Furthermore, wide spread has been observed in the transitional layer (from 20 to 44 km depth) and the upper crust (from 0 to 8 km depth) was not resolved at this stage.

Path B (Figure 5b) shows a shear wave velocity structure slightly different from that observed in path A. In this case, the upper 28 km of the crust seems to be close to the high velocity sedimentary rocks or crystalline basement. Considering that the upper 12 km of the crust was not resolved, it is reasonable to assume that the shear wave velocities are related to the intermediate crust. Again, the transitional layer (β=4.02 km/s) was detected, but here it is thinner than in path A. The crust-mantle transition has been clearly found at 36 km depth. The resolving kernels exhibit the same behavior as in path A, (i.e., a lack of resolution in the upper crust and the best resolution in both the intermediate crust and uppermost mantle).

Path C (Figure 6b) has two strong velocity gradients defining the sediment - lower crust transition (from 1.34 to 3.75 km/s) and the crystalline basement - Moho transition (from 3.20 to 4.86 km/s). This sequence represents a total inversion in the order of the structures. It is important to observe in Figure 6b that no resolution has been achieved in the depth range from 12 to 28 km. The best resolution was observed exactly in the sedimentary layers (from 4 to 12 km). After this, the resolution became relevant both in the depth range from 28 to 36 km and in the half-space.

As described in the previous section, groups of layers with almost similar shear velocities were transformed into thick layers and another inversion process was performed. The results of the inversion procedure are shown in Figures 7-9. Figures 7a, 8a and 9a display both predicted and calculated Rayleigh wave group velocities, while Figures 7b, 8b and 9b display the estimated shear wave velocity structures and corresponding resolving kernels. The estimated shear wave velocities for the three paths are also shown in Table 5.

The upper part (0-20 km depth) of the path A (Figure 7b) has assumed shear velocities close to high velocity sedimentary rocks, which are typical of middle crustal layers (Cloethingh *et al.*, 1979). By analyzing the corresponding resolving kernels (Figure 7b) it is possible to see that the maximum resolution for this part of the model is concentrated in the second layer, and therefore the estimated shear velocity is representative of this depth range. The lower crust, assumed to be the transitional layer (β=4.22 km/s), was well resolved. The Moho boundary was clearly observed at 44 km depth, but no resolution was obtained below this depth (Figure 7b).

In the path B (Figure 8b), only the second layer was resolved. The shear wave velocity associated with this layer (β=3.38 km/s) is typical of high velocity sedimentary rocks. As in path A, both upper crust and uppermost mantle were not resolved, but the crust-mantle transition was clearly observed.

The parametrization of path C was a little different from the other paths because it was necessary to include more layers in order to get a better fit between the theoretical and calculated dispersion curves. As in the first step, only the second and the fifth layers were resolved. The sediment-lower crust transition (from 1.33 to 3.86 km/s) and the crystalline basement-peridotite transition (from 3.16 to 4.78 km/s) were emphasized in the estimated model. The low velocity zone between 28 and

(A)

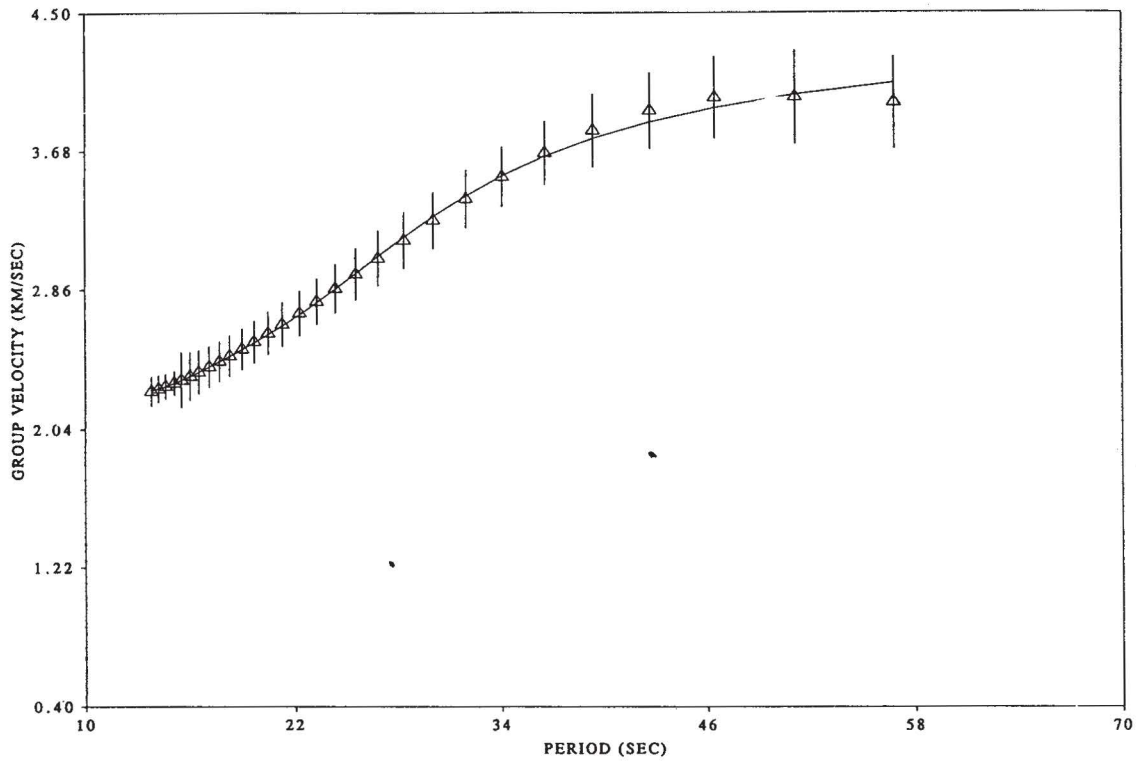

(B)

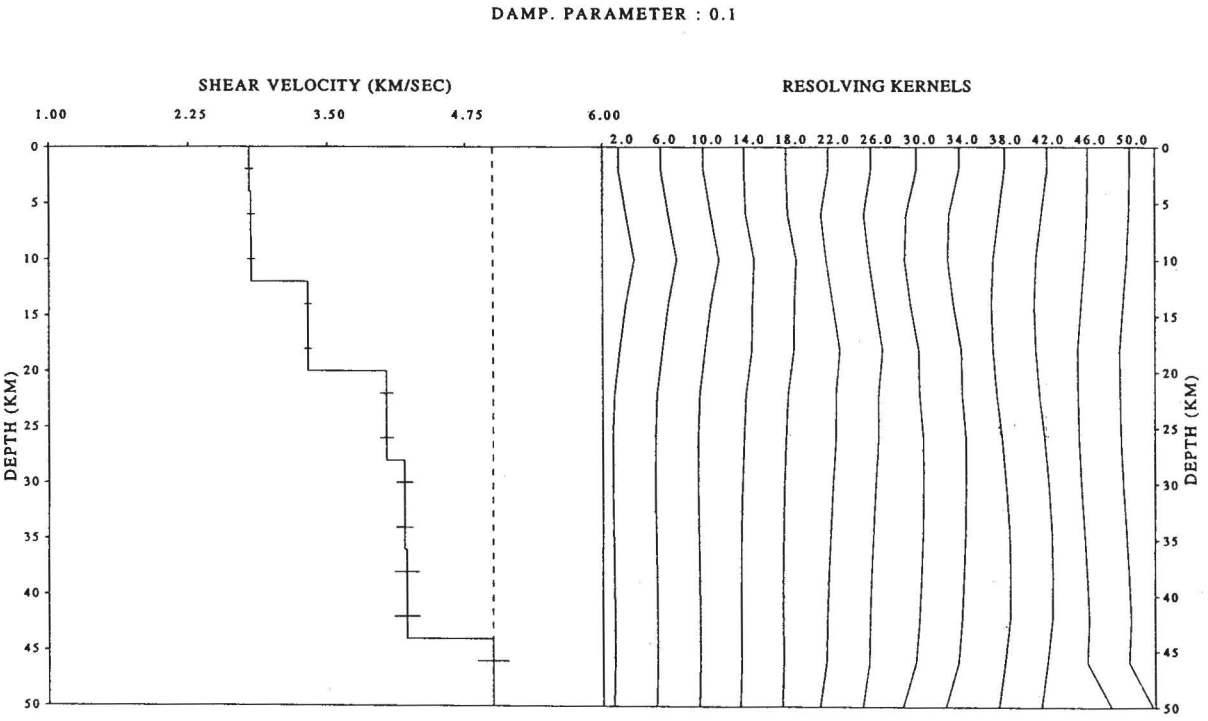

Fig. 4. Inversion results for the first step -path A. (a) Calculated (triangles) and theoretical (solid line) Rayleigh wave group velocities. Vertical bars are the total errors discussed in the text. (b) On the left side are both estimated shear wave velocity structure (solid line) and starting model (dashed line). On the right side are the corresponding resolving kernels to each layer of the model. On the top, the damping parameter value used in the inversion procedure.

(A)

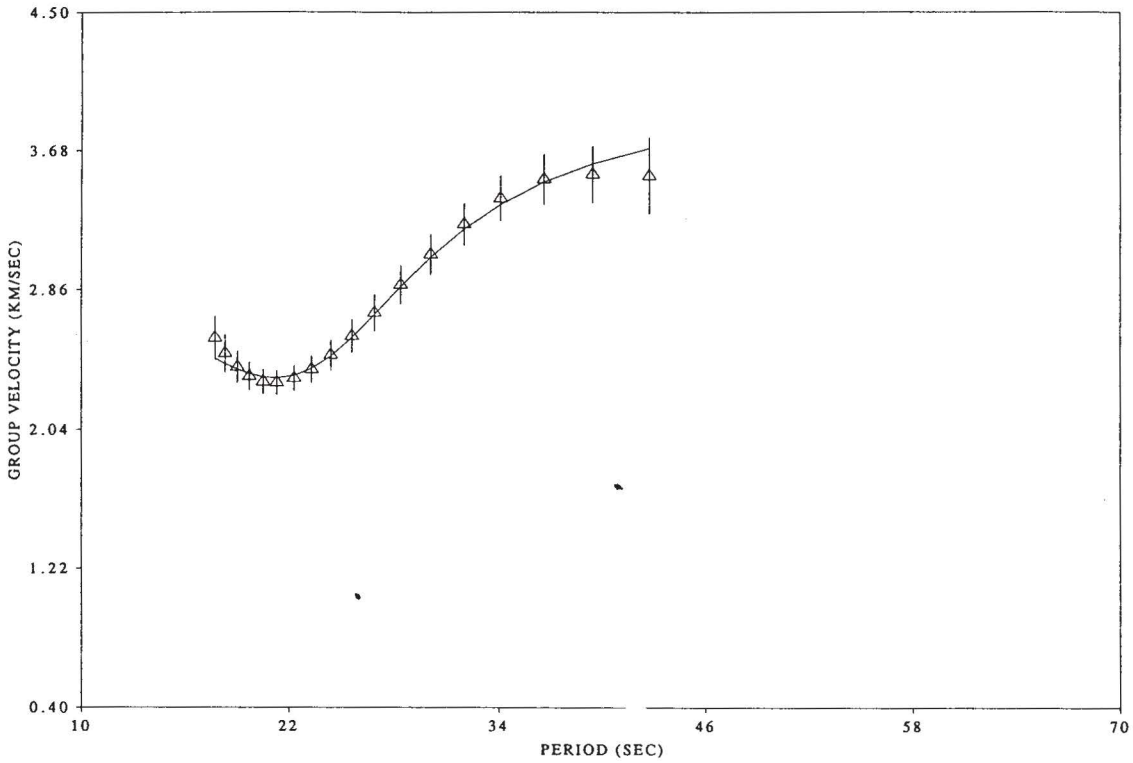

(B)

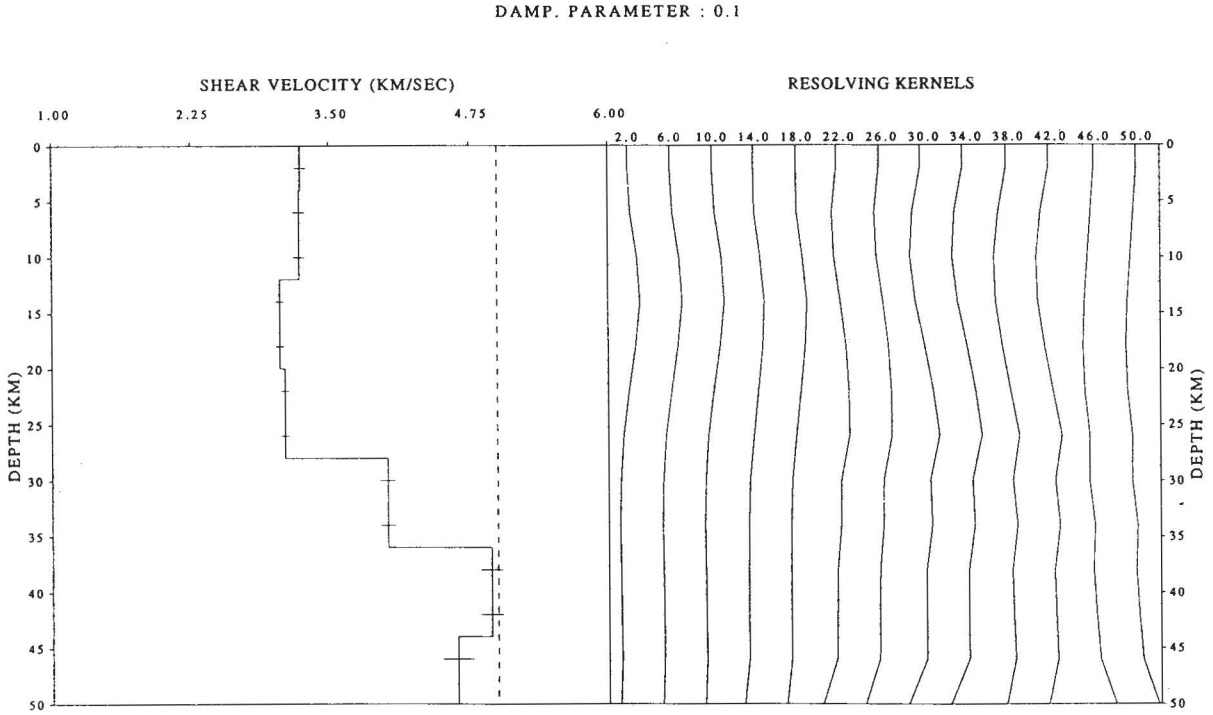

Fig. 5. Inversion results for the first step -path B. (a) Calculated (triangles) and theoretical (solid line) Rayleigh wave group velocities. Vertical bars are the total errors discussed in the text. (b) On the left side are both estimated shear wave velocity structure (solid line) and starting model (dashed line). On the right side are the corresponding resolving kernels to each layer of the model. On the top, the damping parameter value used in the inversion procedure.

Table 3

Rayleigh wave group velocities (U) for the southeastern Brazilian continental margin. e is the total error on group velocities as discussed in the text.

PATH A			PATH B			PATH C		
T (km/s)	U (km/s)	e (km/s)	T (km/s)	U (km/s)	e (km/s)	T (km/s)	U (km/s)	e (km/s)
13.8	2.263	±0.088	17.7	2.579	±0.131	19.7	0.690	±0.048
14.2	2.277	0.080	18.3	2.486	0.112	20.1	0.674	0.042
14.6	2.292	0.075	19.0	2.406	0.095	20.5	0.665	0.037
15.1	2.312	0.071	19.7	2.352	0.083	20.9	0.664	0.032
15.5	2.329	0.162	20.5	2.320	0.075	21.3	0.669	0.029
16.0	2.351	0.141	21.3	2.315	0.073	21.8	0.683	0.027
16.5	2.375	0.129	22.3	2.340	0.075	22.3	0.707	0.026
17.1	2.405	0.122	23.3	2.393	0.082	22.8	0.738	0.025
17.7	2.437	0.119	24.4	2.476	0.091	23.3	0.777	0.025
18.3	2.470	0.121	25.6	2.588	0.100	23.8	0.822	0.025
19.0	2.510	0.122	26.9	2.724	0.109	24.4	0.885	0.026
19.7	2.553	0.124	28.4	2.888	0.115	25.0	0.955	0.026
20.5	2.603	0.126	30.1	3.067	0.120	25.6	1.032	0.031
21.3	2.655	0.131	32.0	3.246	0.124	26.3	1.129	0.027
22.3	2.721	0.133	34.1	3.400	0.134	26.9	1.217	0.035
23.3	2.790	0.138	36.6	3.512	0.148	27.7	1.341	0.033
24.4	2.867	0.146	39.4	3.542	0.168	28.4	1.453	0.036
25.6	2.952	0.155	42.7	3.532	0.227	29.3	1.601	0.036
26.9	3.045	0.164			0.281	30.1	1.735	0.040
28.4	3.151	0.168				31.0	1.887	0.042
30.1	3.269	0.170				32.0	2.054	0.047
32.0	3.396	0.173				33.0	2.217	0.053
34.1	3.527	0.179				34.1	2.391	0.067
36.6	3.668	0.190				35.3	2.572	0.082
39.4	3.801	0.218				36.6	2.755	0.108
42.7	3.918	0.227				37.9	2.923	0.108
46.5	3.995	0.245				39.4	3.096	0.113
51.2	3.997	0.278				41.0	3.257	0.114
56.9	3.964	0.273				42.7	3.400	0.106
						44.5	3.523	0.113
						46.5	3.629	0.143
						48.8	3.718	0.137
						51.2	3.784	0.145
						53.9	3.843	0.170
						56.9	3.907	0.156
						60.2	3.999	0.192
						64.0	3.981	0.176

36 km depth was necessary to obtain a reasonable fit between theoretical and calculated dispersion curves. This layer was clearly resolved (Figure 9b), but in terms of structure, it represents an inversion of the normal sequence

(A)

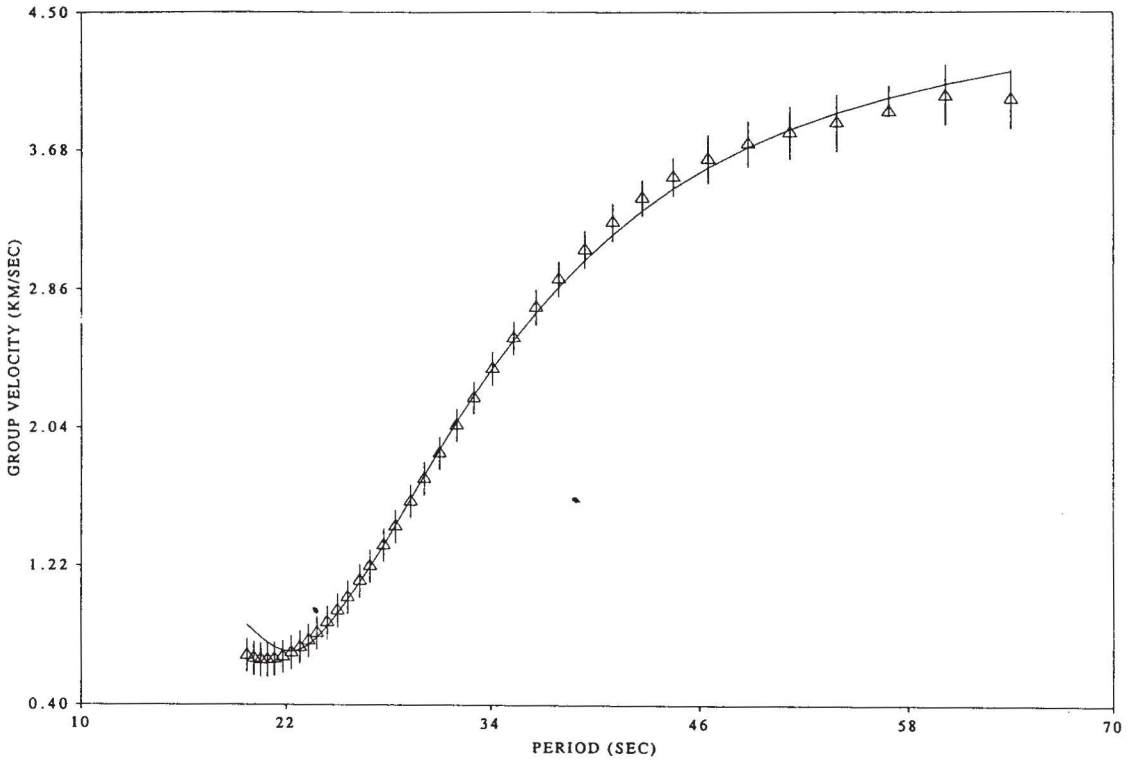

(B)

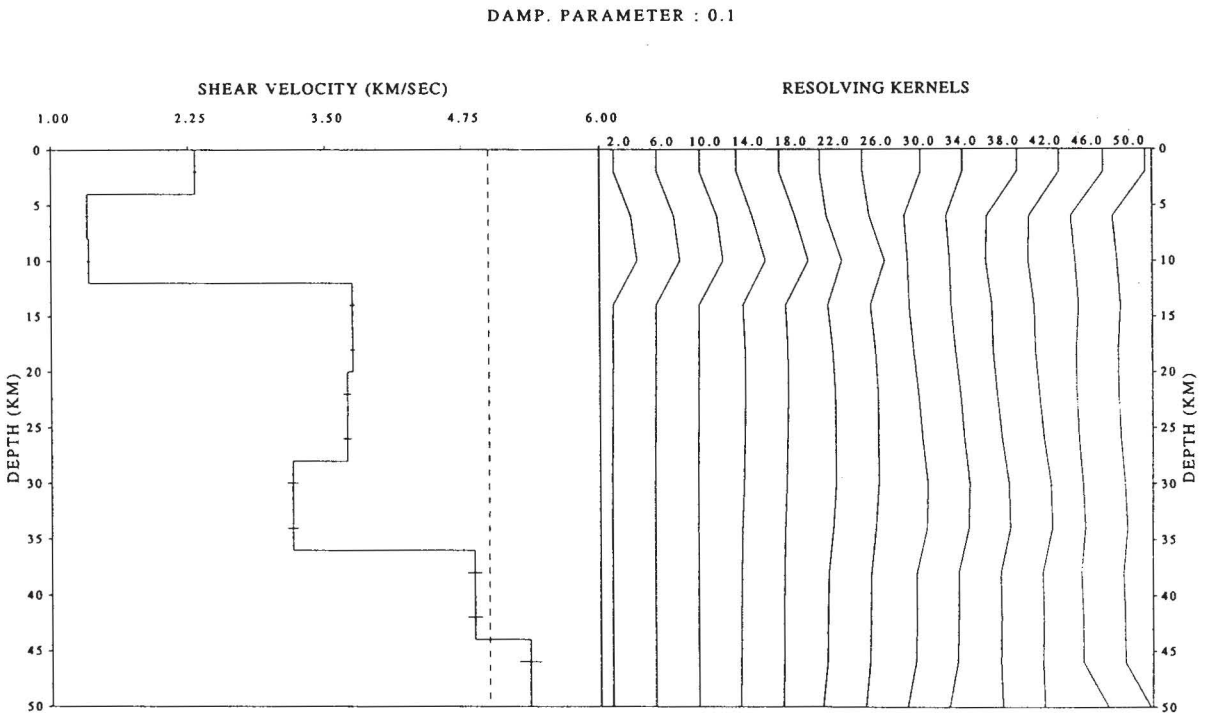

Fig. 6. Inversion results for the first step -path C. (a) Calculated (triangles) and theoretical (solid line) Rayleigh wave group velocities. Vertical bars are the total errors discussed in the text. (b) On the left side are both estimated shear wave velocity structure (solid line) and starting model (dashed line). On the right side are the corresponding resolving kernels to each layer of the model. On the top, the damping parameter value used in the inversion procedure.

(A)

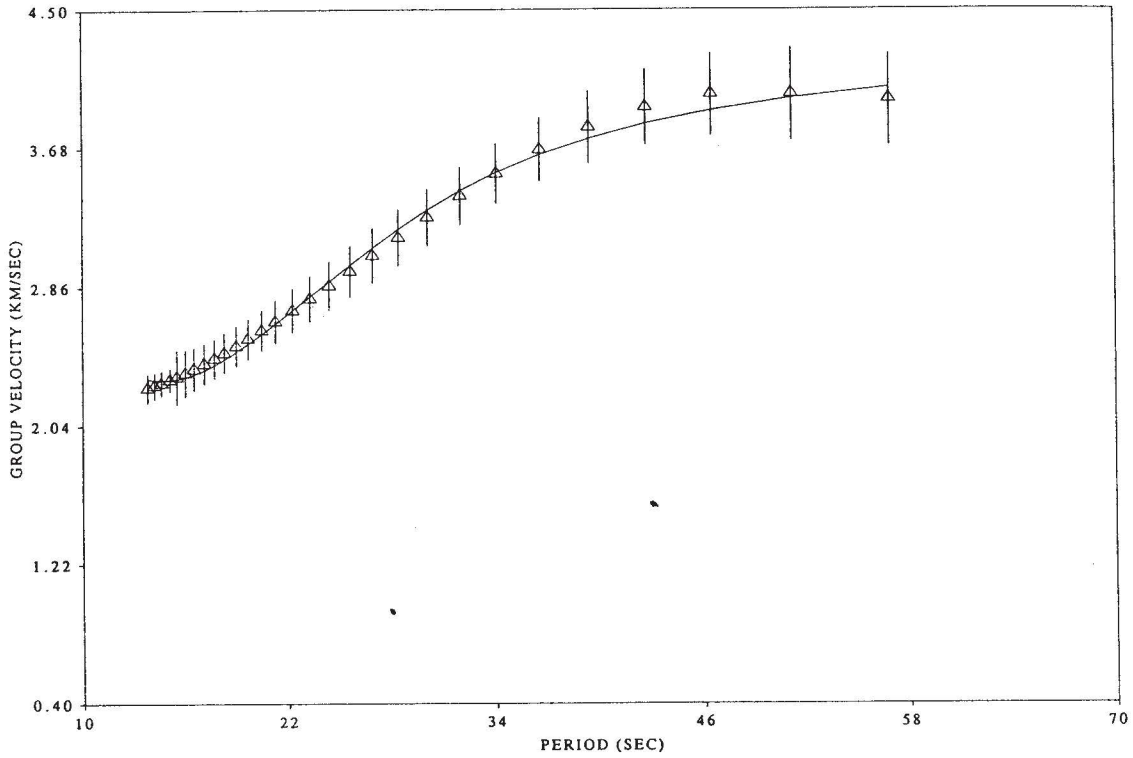

(B)

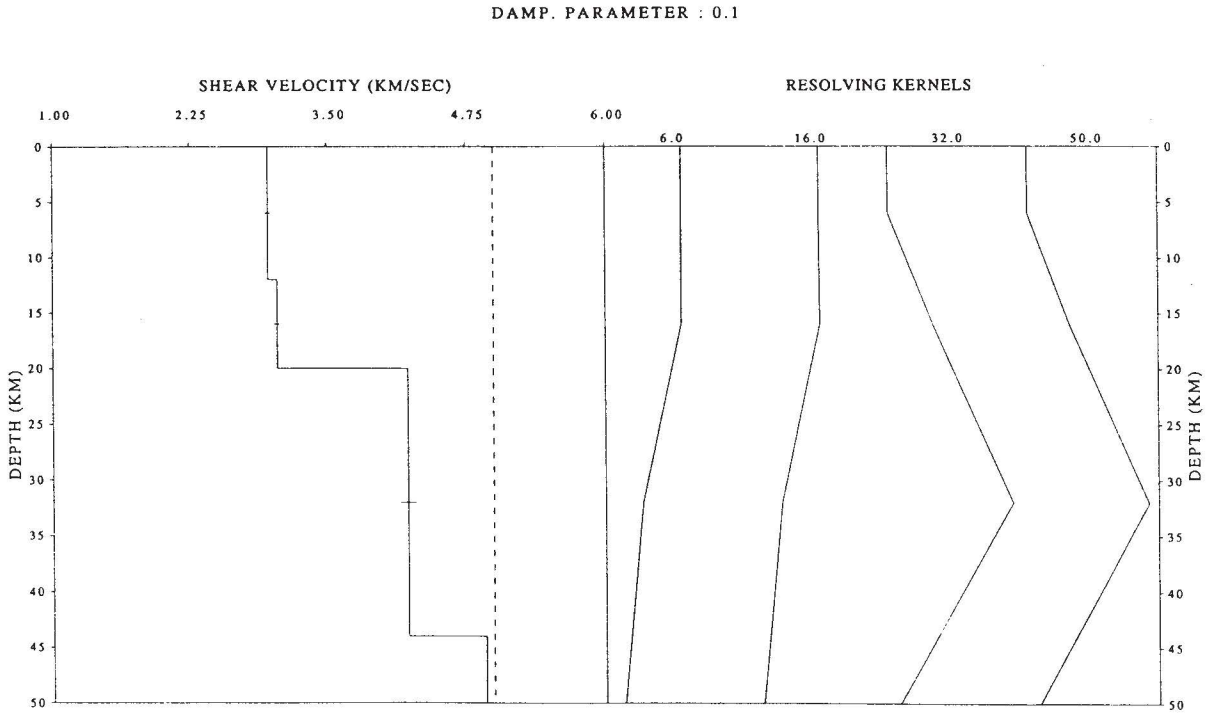

Fig. 7. Inversion results for the second step -path A. (a) Calculated (triangles) and theoretical (solid line) Rayleigh wave group velocities. Vertical bars are the total errors discussed in the text. (b) On the left side are both estimated shear wave velocity structure (solid line) and starting model (dashed line). On the right side are the corresponding resolving kernels to each layer of the model. On the top, the damping parameter value used in the inversion procedure.

Table 4

Estimated shear wave velocity structures obtained in the first step of the inversion process. H is thickness, β is shear wave velocity and σ is the standard deviation of estimated parameters.

PATH A			PATH B			PATH C		
H (km)	β (km/s)	σ (km/s)	H (km)	β (km/s)	σ (km/s)	H (km)	β (km/s)	σ (km/s)
4.0	2.80	0.04	4.0	3.24	0.05	4.0	2.31	0.02
4.0	2.81	0.04	4.0	3.23	0.05	4.0	1.32	0.02
4.0	2.81	0.04	4.0	3.23	0.05	4.0	1.34	0.02
4.0	3.32	0.03	4.0	3.06	0.04	4.0	3.75	0.03
4.0	3.32	0.03	4.0	3.06	0.04	4.0	3.75	0.03
4.0	4.03	0.06	4.0	3.10	0.04	4.0	3.70	0.04
4.0	4.03	0.06	4.0	3.10	0.04	4.0	3.70	0.04
4.0	4.19	0.08	4.0	4.02	0.07	4.0	3.20	0.05
4.0	4.19	0.08	4.0	4.02	0.07	4.0	3.20	0.05
4.0	4.22	0.12	4.0	4.94	0.10	4.0	4.86	0.07
4.0	4.22	0.12	4.0	4.94	0.10	4.0	4.86	0.07
4.0	5.00	0.14	4.0	4.64	0.14	4.0	5.36	0.10
∞	5.00	0.14	∞	4.64	0.14	∞	5.36	0.10

Table 5

Estimated shear wave velocity structures for the second step of the inversion process. H is the thickness, β is shear wave velocity and σ is the standard deviation on estimated S wave velocities.

PATH A			PATH B			PATH C		
H (km)	β (km/s)	σ (km/s)	H (km)	β (km/s)	σ (km)	H (km)	β (km/s)	σ (km/s)
12.0	2.97	0.03	12.0	2.89	0.02	4.0	2.36	0.02
8.0	3.05	0.03	16.0	3.38	0.02	8.0	1.33	0.02
24.0	4.22	0.07	8.0	3.62	0.02	8.0	3.86	0.07
∞	4.92	0.07	∞	4.96	0.06	8.0	3.81	0.07
						8.0	3.16	0.06
						8.0	4.78	0.06
						∞	5.38	0.05

used to characterize continental shelf regions (Cloetingh *et al.*, 1979). Both the upper crust and half-space were not resolved, but the crust-mantle transition was perfectly defined at 36 km depth.

In order to identify common features between the estimated shear wave velocities, all estimated models were compared to the one (CS-continental shelf) found by Souza (1995) in the same area (Figure 10). In the upper crust, two situations were identified. The first one is that models C and CS are in agreement with respect to the sedimentary layer. The second one is an agreement between both models A and B, but these models are not well resolved at this depth range. Between 12 and 28 km depth, models B and CS are closer to one another, along with a slight approximation of model A in the first 8 km. In this depth range, model A is not properly resolved. Between 28 and 36 km depth, models C and CS are quite compatible. In spite of the half-space not being well resolved, the Moho boundary is clearly identified in all inversion results. Finally, a reduction in the crustal thickness is observed from path A to path C (Figure 10).

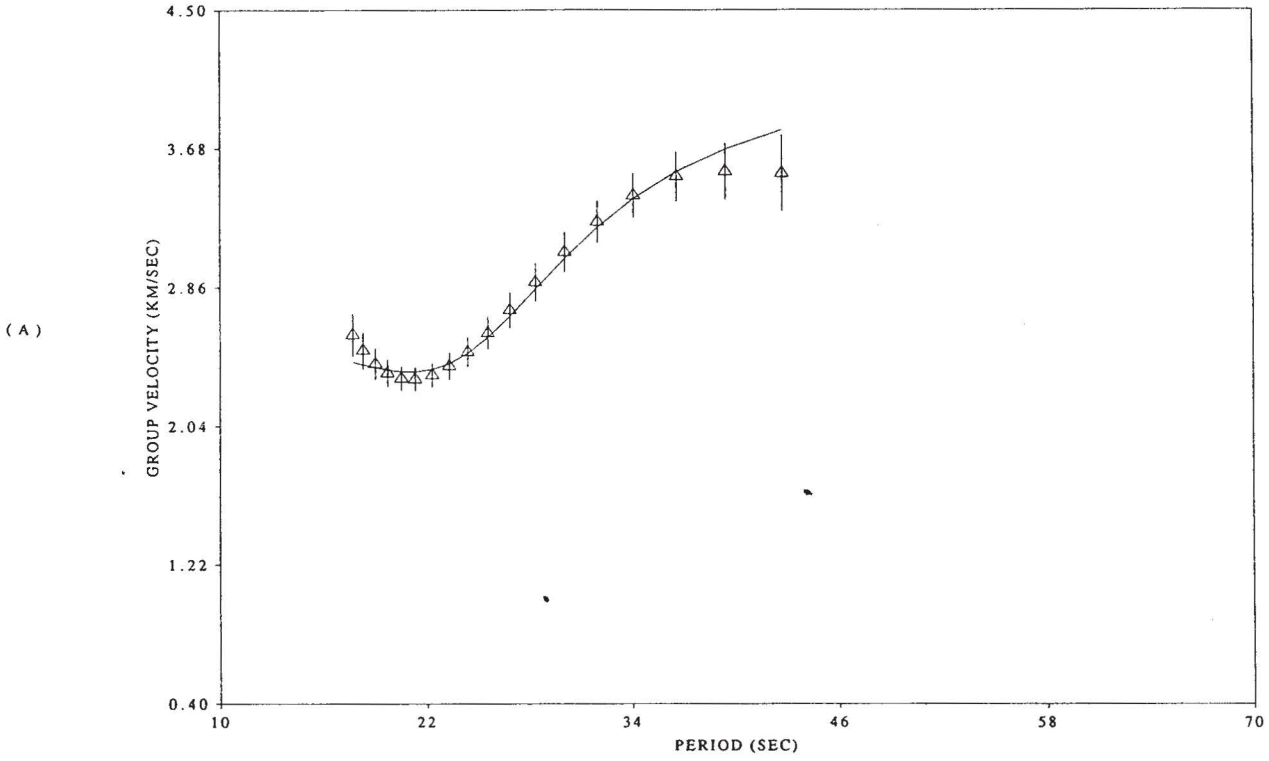

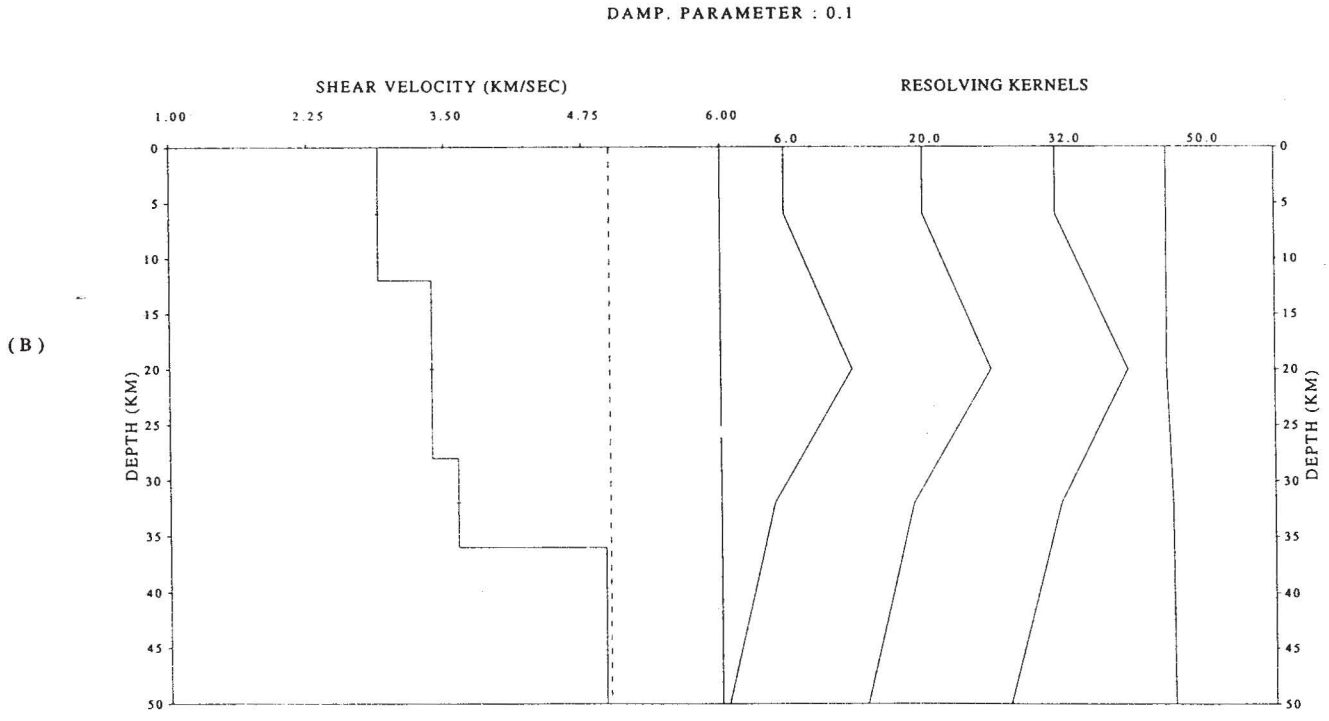

Fig. 8. Inversion results for the second step -path B. (a) Calculated (triangles) and theoretical (solid line) Rayleigh wave group velocities. Vertical bars are the total errors discussed in the text. (b) On the left side are both estimated shear wave velocity structure (solid line) and starting model (dashed line). On the right side are the corresponding resolving kernels to each layer of the model. On the top, the damping parameter value used in the inversion procedure.

(A)

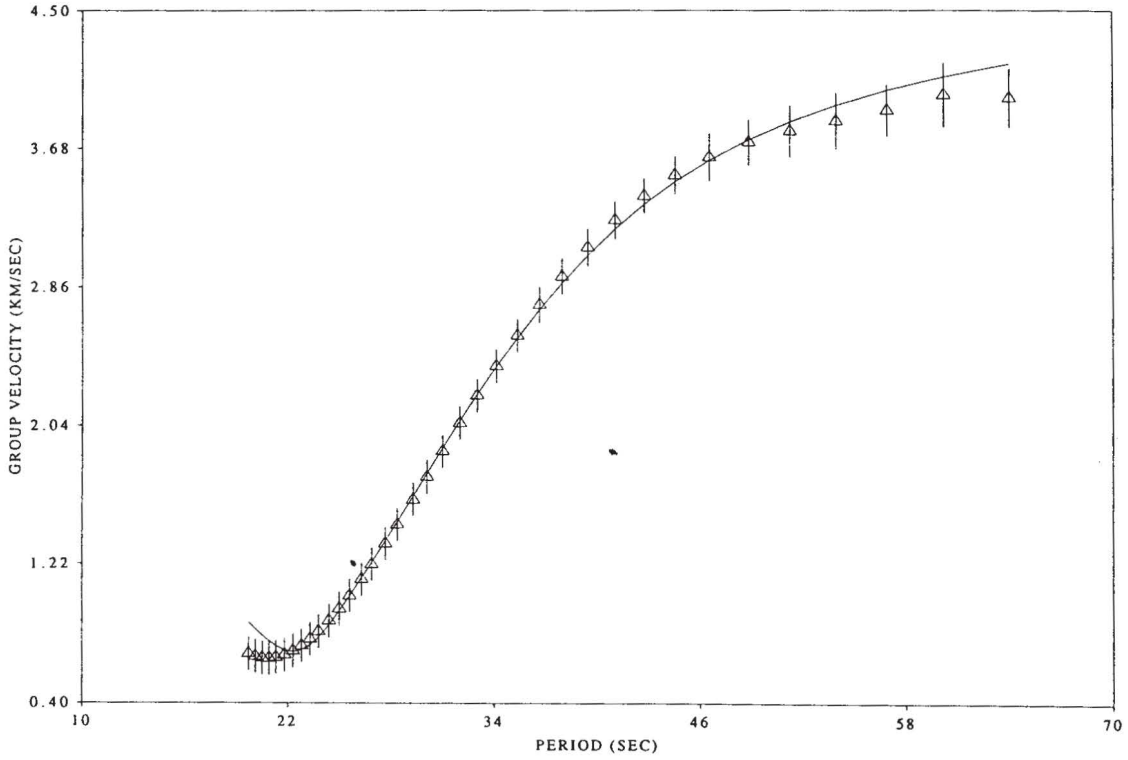

(B)

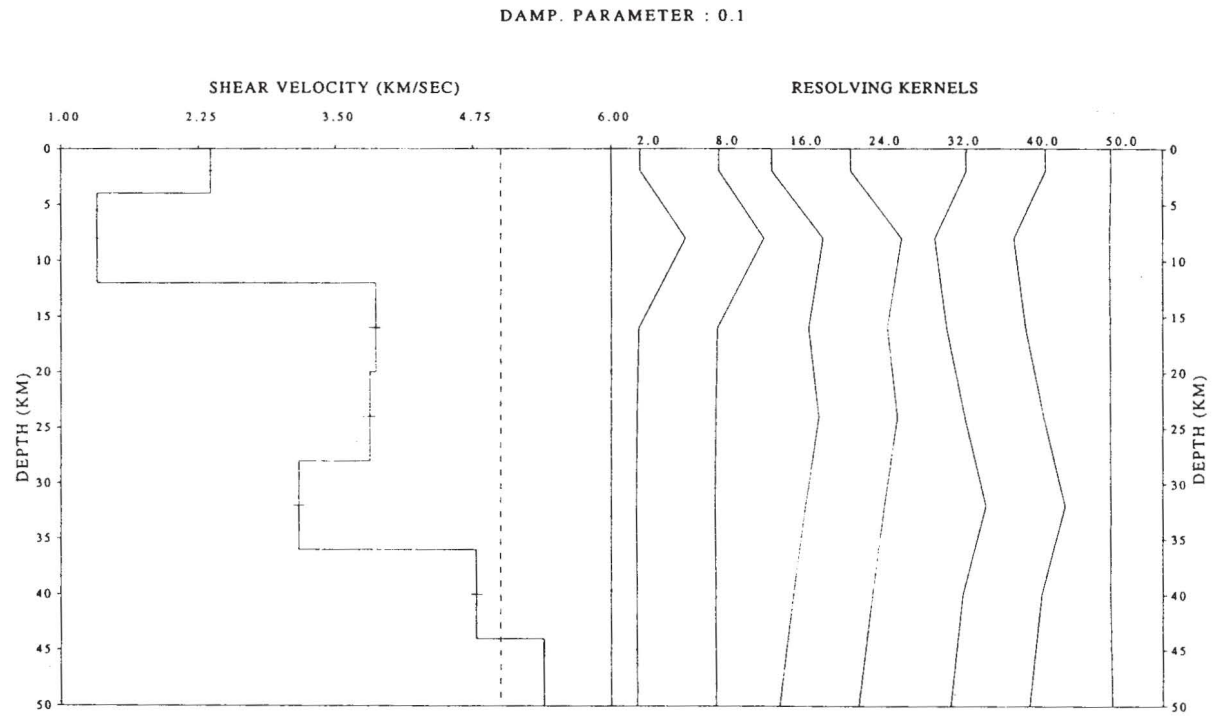

Fig. 9. Inversion results for the second step -path C. (a) Calculated (triangles) and theoretical (solid line) Rayleigh wave group velocities. Vertical bars are the total errors discussed in the text. (b) On the left side are both estimated shear wave velocity structure (solid line) and starting model (dashed line). On the right side are the corresponding resolving kernels to each layer of the model. On the top, the damping parameter value used in the inversion procedure.

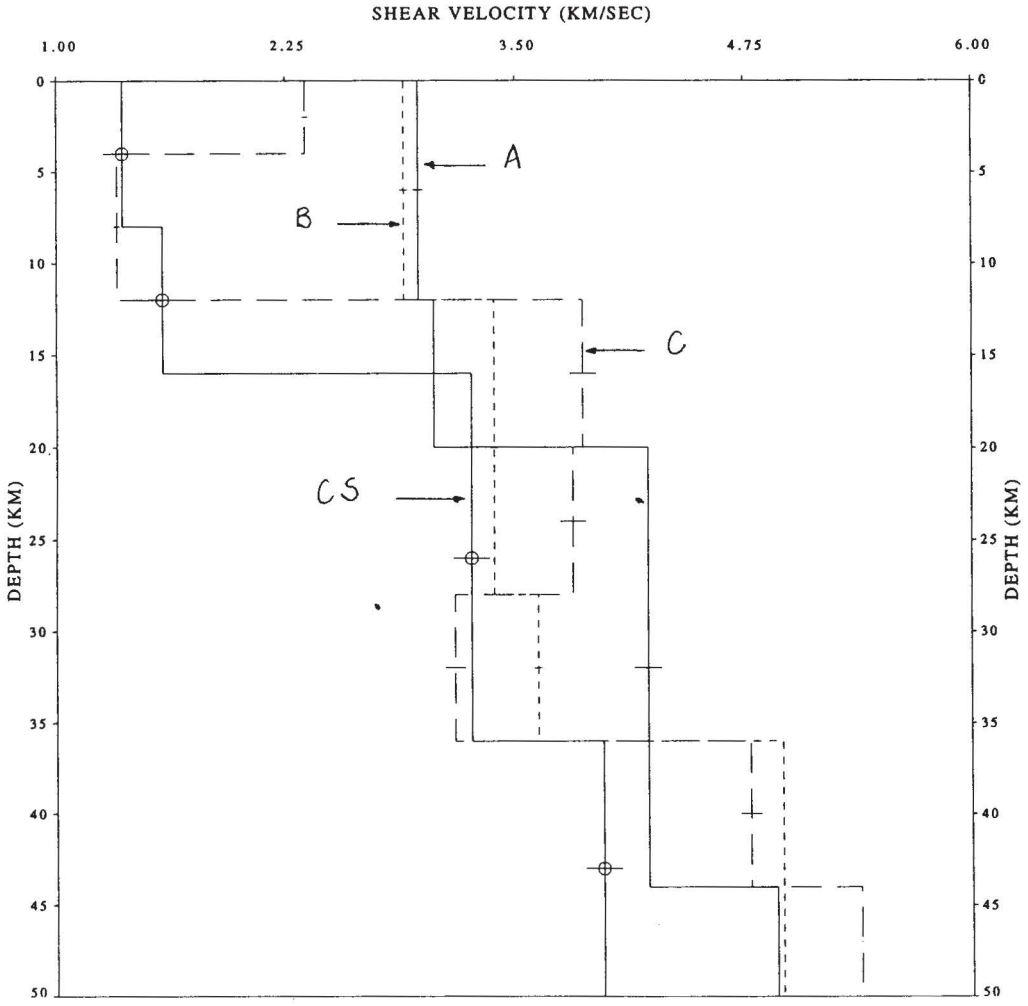

Fig. 10. Comparison between the S-wave velocity structures obtained in the present study (A, B and C) and that (CS- Continental Shelf) found by Souza (1995). The horizontal bars are the standard deviations shown in Table 5.

CONCLUSIONS

Rayleigh wave group velocities obtained at Brazilian seismological station RDJ have been used to study the crustal structure of the southeastern Brazilian continental shelf along three paths. The source-station paths have been divided into two types of structures, so that the dispersion curves corresponding to continental shelf have been calculated. Inversion results of the continental shelf dispersion curves indicate that the upper crust is dominated by sediments and high velocity sedimentary rocks with shear wave velocities varying from 1.32 to 2.90 km/s. The intermediate crust has assumed shear velocities ($3.06 \leq \beta \leq 3.38$ km/s) typical of crystalline basement. The lower crust seems to be composed of a transitional layer ($4.02 \leq \beta \leq 4.22$ km/s), such as is observed in other passive continental margins (Dainty *et al.*, 1966; Calcagnile *et al.*, 1982). This layer is also in agreement with a recent surface wave study in the same area (Souza, 1995). From path A to C, it is possible to verify a reduction in the total crustal thickness. The crust-mantle transition is well defined at 36±4 km depth, except in the path A where it reaches 44 km depth.

ACKNOWLEDGMENTS

The author would like to thank CNPq/Observatório Nacional for financial support to take part in the Regional Seismological Assembly in South America. Special thanks to Constantino de Mello Mota and Elisabeth da Cunha Lima for the digitization of the magnetic lineations on the sea-floor used in Figure 1.

BIBLIOGRAPHY

ANDERSON, D. L. and R. S. HART, 1976. An earth model based on free oscillations and body waves. *J. Geophys. Res., 81,* 1461-1475.

BIRCH, F., 1964. Density and composition of mantle and core. *J. Geophys. Res., 69,* 4377-4388.

CALCAGNILE, G., F. D'INGEO, P. FARRUGIA and G. P. PANZA, 1982. The lithosphere in the central-east-

ern Mediterranean area. *Pure and Appl. Geophys., 120,* 389-406.

CANAS, J.A. and B.J. MITCHELL, 1981. Rayleigh wave attenuation and its variation across Atlantic Ocean. *Geophys. J. R. Astr. Soc., 67,* 159-179.

CHAVE, A.D., 1979. Lithospheric structure of the Walvis ridge from Rayleigh wave dispersion. *J. Geophys. Res., 84,* 6840-6848.

CHRISTENSEN, D.H., J.K. KIMBALL and F.J. MAUK, 1980. Rayleigh wave group velocity dispersion in the North and South Atlantic Oceans. *Bull. Seism. Soc. Am., 70,* 1787-1809.

CLOETINGH, S., G. NOLET and R. WORTEL, 1979. On the use of Rayleigh wave group velocities for the analysis of continental margins. *Tectonophysics, 59,* 335-346.

DAINTY, A. M., C. E. KEEN, M. J. KEEN and J. E. BLANCHARD, 1966. Review of geophysical evidence on crust and upper-mantle structure on the seaboard of Canada. *Amer. Geophys. Union Mono. Ser., 10,* 349-369.

DZIEWONSKI, A., S. BLOCH and M. LANDISMAN, 1969. A technique for the analysis of transient seismic signals. *Bull. Seism. Soc. Am., 59,* 427-444.

DZIEWONSKI, A. M., 1971. Upper mantle models from 'pure-path' dispersion data. *J. Geophys. Res., 76,* 2587-2601.

EMERY, K. O. and E. UCHUPI, 1984. The geology of the Atlantic Ocean. Springer-Verlag, New York.

FORSYTH, D. W., 1975. The early structural evolution and anisotropy of the oceanic upper mantle. *Geophys. J. R. Astr. Soc., 43,* 103-162.

HERRMANN, R.B., 1991. Computer programs for Seismology, vol. IV, St. Louis University, St. Louis, MO.

HONDA, S. and T. TANIMOTO, 1987. Regional 3-D heterogeneities by waveform inversion-application to the Atlantic area. *Geophys. J. R. Astr. Soc., 91,* 737-753.

KANAMORI, H., 1970. Velocity and Q for mantle waves. *Phys. Earth. Planet. Inter., 2,* 259-275.

MOCQUET, A., B. ROMANOWICZ and J.P. MONTAGNER, 1989. Three-dimensional structure of the upper mantle beneath the Atlantic Ocean inferred from long-period Rayleigh waves: 1. Group and phase velocity distributions. *J. Geophys. Res., 94,* 7449-7468.

MOCQUET, A. and B. ROMANOWICZ, 1990. Three-dimensional structure of the upper mantle beneath the Atlantic Ocean inferred from long-period Rayleigh waves: 2. Inversion. *J. Geophys. Res., 95,* 6787-6798.

SANTÔ, T. A., 1960. Observations of surface waves by Columbia-type seismograph installed at Tsukuba station, Japan (Part I) - Rayleigh wave dispersions across the oceanic basin. *Bull. Earthq. Res. Inst., 38,* 219-240.

SANTÔ, T. and M. BATH, 1963. Crustal structure of Pacific Ocean area from dispersion of Rayleigh waves. *Bull. Seism. Soc. Am., 53,* 151-165.

SOUZA, J. L. de, 1994. S wave velocity in the South Atlantic Ocean lithosphere, submitted to Anais Acad. Bras. Cienc., in press.

SOUZA, J. L. de, 1995. Shear wave velocity in the southeastern Brazilian continental shelf. *Geophys. J. Int., 122,* 691-702.

TALWANI, M., G. H. SUTTON and J. L. WORTZEL, 1959. A crustal section across the Puerto Rico trench. *J. Geophys. Res., 64,* 1545-1555.

TARKOV, A. P. and V. V. VAVAKIN, 1982. Poisson's ratio behaviour in various crystalline rocks: application to the study of the earth's interior. *Phys. Earth. Planet. Inter., 29,* 24-29.

WEIDNER, D. J., 1974. Rayleigh wave phase velocities in the Atlantic Ocean. *Geophys. J. R. Astr. Soc., 36,* 105-139.

Jorge Luis de Souza
Observatório Nacional, Departamento de Geofísica
R. Gal. José Cristino, 77-São Cristovão
20921-400 Rio de Janeiro, Brasil.